DOI: 10.1002/ejic.200700465

Reactions of 1,2,4-Trithiolanes with Nonacarbonyldiiron: Sulfurdithiolatodiiron and -tetrairon Complexes as Mimics for the Active Site of [Fe-only] Hydrogenase

Jochen Windhager,[a] Helmar Görls,[a] Holm Petzold,[a] Grzegorz Mloston,[b] Gerald Linti,*[c] and Wolfgang Weigand*[a]

Dedicated to Prof. Dieter Seebach on the occasion of his 70th birthday

Keywords: Iron / Cluster compounds / S ligands / Hydrogenases / Density functional calculations

The reactions of 1,2,4-trithiolane (**1a**), 3,3,5,5-tetramethyl-1,2,4-trithiolane (**1b**), 3,3,5,5-tetraethyl-1,2,4-trithiolane (**1c**), 3,3,5,5-bis(pentamethylene)-1,2,4-trithiolane (**1d**) and dispiro{tricyclo[3.3.1.1]decane-2,3′′-(1,2,4)-trithiolane-5′,2′-tricyclo[3.3.1.1]decane} (**1e**) with nonacarbonyldiiron (**2**) have been investigated. The sulfurdithiolatodiiron complexes **3a–e**, which can be considered as novel model complexes of the active site of the [Fe-only] hydrogenase, were isolated as the main products of these reactions. X-ray structure analyses were performed on compounds **3b–e**. The carbon dithiolato (SCR_2S)-bridged diiron side-products **4a–e** and the tetranuclear clusters **6b–d** were also obtained and characterised by X-ray diffraction analysis (**4b–e** and **6b–d**). In contrast, the reaction of **1e** with **2** affords the trinuclear complex **7**, which contains a side-on bonded adamantanethione, besides **3e** and **4e**. Finally, the reaction of **3a** with two equivalents of $(Et_4N)CN$ gives the monocyanide complex **8** in good yield. Density functional calculations have been performed to evaluate the bonding situation in the di- and tetranuclear clusters.

Introduction

The oxidative addition of platinum(0) complexes to cyclic disulfides has received significant attention during the last few years.[1] We have recently investigated reactions of 1,2,4-trithiolanes with platinum(0) complexes, which lead to the insertion of the platinum(0) complex fragment into the S–S bond,[2] and have also shown that 1,2,4-trithiolane (**1a**) can be added oxidatively to $[Fe_2(CO)_9]$ (**2**) to give the sulfurdithiolatodiiron (SDT) complex $[Fe_2(\mu\text{-}SCH_2SCH_2S\text{-}\mu)(CO)_6]$ (**3a**) as well as $[Fe_2(\mu\text{-}SCH_2S\text{-}\mu)(CO)_6]$ (**4a**).[3,4] Similar reactions involving $[Fe_3(CO)_{12}]$ and **1a**, which lead to complex **3a**, have been reported recently.[3c]

Since publication of the first X-ray structure determination of the [Fe-only] hydrogenase,[6] numerous model compounds for the active site of the enzyme, such as propanedithiolato- (PDT),[7a–7d] azadithiolato- (ADT)[7e–7g] and oxadithiolatodiiron (ODT) derivatives, have been described (Scheme 1).[7f,7i,7l]

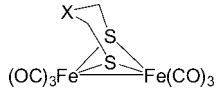

Scheme 1. Model complexes for the active site of [Fe-only] hydrogenase with X = CH_2, NH, O and S.

In the light of recent results, reactions of iron carbonyls with sulfur-rich heterocycles such as 1,2,4-trithiolanes could offer a new approach to the synthesis of products related to [Fe-only] hydrogenase. To the best of our knowledge, reactions of 1,2,4-trithiolane derivatives with iron carbonyls have seldom been described.[3c,3d]

Here we describe the reactions of tetrasubstituted 1,2,4-trithiolanes **1a–e** (Scheme 2) with $[Fe_2(CO)_9]$ (**2**) as a systematic investigation of the influence of the substituents' size on the molecular structure of the products. Density functional calculations for one complex are also reported.

[a] Institut für Anorganische und Analytische Chemie, Friedrich-Schiller-Universität Jena,
August-Bebel-Strasse 2, 07743 Jena, Germany
Fax: +49-3641-948-102
E-Mail: c8wewo@uni-jena.de
[b] Section of Heteroorganic Compounds, University of Lodz,
Narutowicza 68, 90–136 Lodz, Poland
Fax: +48-42-678-1609
E-mail: gmloston@uni.lodz.pl
[c] Anorganisch-Chemisches Institut, Ruprecht-Karls-Universität Heidelberg,
Im Neuenheimer Feld 270, 69120 Heidelberg, Germany
Fax: +49-6221-54-66-17
E-mail: gerald.linti@aci.uni-heidelberg.de

Supporting information for this article is available on the WWW under http://www.eurjic.org or from the author.

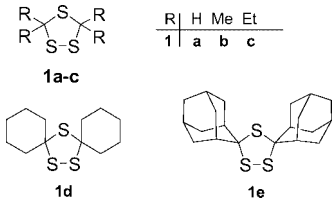

Scheme 2. 1,2,4-Trithiolanes **1a**–**e**.

Results and Discussion

Reactions of 1,2,4-Trithiolanes (1a–d) with [$Fe_2(CO)_9$] (2)

Three equivalents of nonacarbonyldiiron (**2**) were treated with one equivalent of the corresponding 1,2,4-trithiolane **1a**–**d** (Scheme 2) for five hours at room temperature in thf to afford a mixture of four compounds of type **3**, **4**, **5** and **6** (Scheme 3), which were isolated by column chromatography. Compounds **3a**,[3] **4a**[4] and **5**[5] have already been described. Complex **6a** was formed at room temperature exclusively but not in the reaction performed at 65 °C.

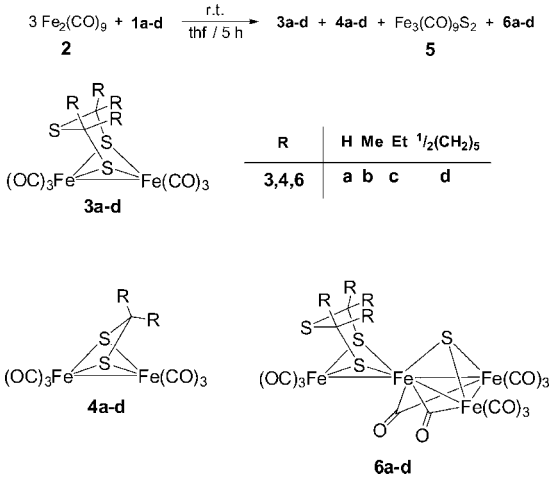

Scheme 3. Reactions of 1,2,4-trithiolanes **1a**–**d** with [$Fe_2(CO)_9$].

The ^{1}H NMR spectra of **3b**,**c** and **4b**,**c** show that the corresponding alkyl groups (R = Me, Et) are chemically equivalent. Furthermore, the $^{13}C\{^1H\}$ NMR spectra display one signal for four methyl groups in **3b** and two signals for four ethyl groups in **3c**. The $^{13}C\{^1H\}$ NMR spectrum of complex **3d** contains three resonance signals at δ = 22.80, 25.23 and 43.22 ppm, respectively, which were attributed to the pentamethylene moiety. The ^{1}H and $^{13}C\{^1H\}$ NMR spectra of **4b**–**d** indicate that the R groups bonded to the bridging carbon atoms (SCR_2S) are equivalent. The mass spectra of **3b**–**d** and **4b**–**d** show the molecular peaks (see Experimental Section) and stepwise fragmentation of six CO groups similar to **3a** and **4a**. Finally, X-ray diffraction analysis confirmed the formation of the dithiolatodiiron complexes **3b**–**d** (Figures 1, 2 and 3, respectively) and **4b**–**d** (see Figures S1–S3 in the electronic supporting information).

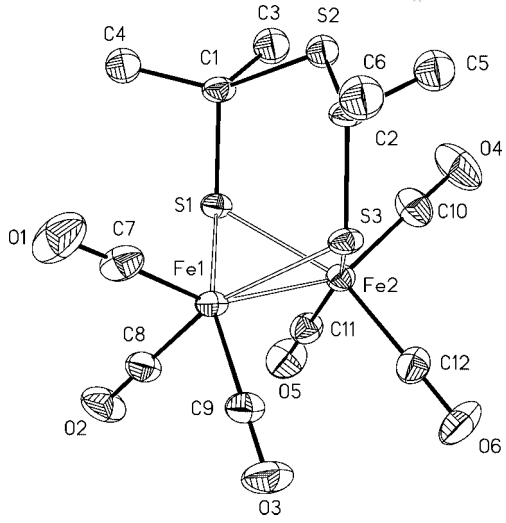

Figure 1. Structure of [$Fe_2\{SC(CH_3)_2SC(CH_3)_2S\}(CO)_6$] (**3b**) showing thermal ellipsoids at the 50% probability level (hydrogen atoms have been omitted for clarity). Selected distances [Å] and angles [°]: Fe(1)–Fe(2) 2.5219(6), Fe(2)–C(7) 1.792(4), Fe(2)–C(8) 1.793(3), Fe(2)–C(9) 1.799(3), Fe(1)–S(1) 2.2495(8), Fe(1)–S(3) 2.2480(9); Fe(1)–S(1)–Fe(2) 68.12(3), Fe(1)–S(3)–Fe(2) 68.18(3).

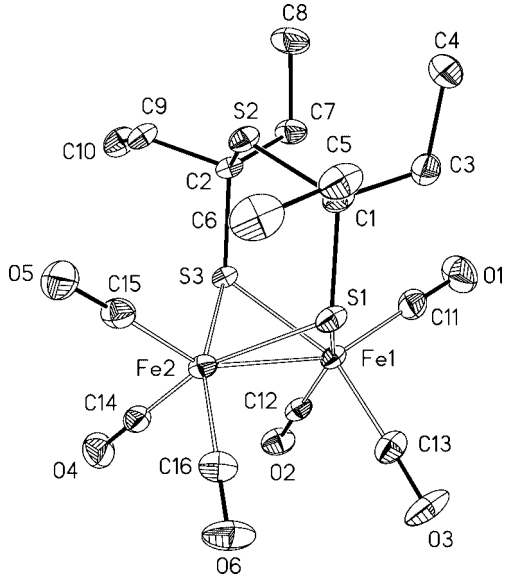

Figure 2. Structure of [$Fe_2\{SC(CH_2CH_3)_2SC(CH_2CH_3)_2S\}(CO)_6$] (**3c**) showing thermal ellipsoids at the 50% probability level (hydrogen atoms have been omitted for clarity). Selected distances [Å] and angles [°]: Fe(1)–Fe(2) 2.5151(4), Fe(1)–C(11) 1.804(2), Fe(1)–C(12) 1.7960(19), Fe(1)–C(13) 1.793(2), Fe(1)–S(1) 2.2648(5), Fe(1)–S(3) 2.2481(5); Fe(1)–S(1)–Fe(2) 67.469(15), Fe(1)–S(3)–Fe(2) 68.055(16).

The iron coordination geometry in **3b**–**d** is rather similar to the sulfurdithiolato (SDT) analogue [$Fe_2(\mu$-SCH_2SCH_2S-$\mu)(CO)_6$] (**3a**).[3] The Fe–Fe bond lengths found in **3b**–**d** are between 2.5151 and 2.5288 Å, slightly longer than those in the corresponding PDT [2.5103(11) Å],[7a–7d] ODT [2.5113(13) Å],[7f,7i,7l] ADT [2.4924(7) Å][7e–7g] and SDT analogs [2.5120(5) Å].[3] Simi-

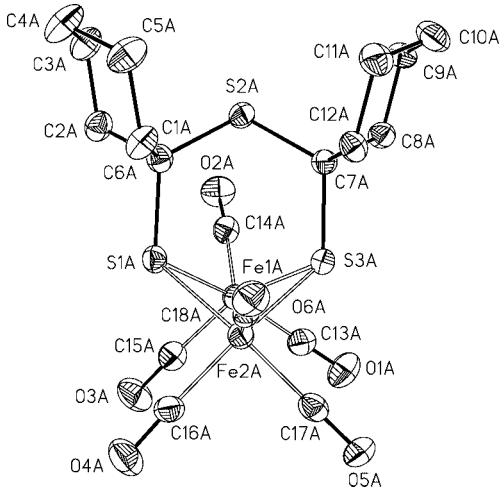

Figure 3. Structure of $[Fe_2\{SC(CH_2)_5SC(CH_2)_5S\}(CO)_6]$ (**3d**) showing thermal ellipsoids at the 50% probability level (hydrogen atoms have been omitted for clarity). Selected distances [Å] and angles [°]: Fe(1A)–Fe(2A) 2.5288(13), Fe(1A)–C(A13) 1.787(8), Fe(A1)–C(A14) 1.819(6), Fe(A1)–C(A15) 1.790(7), Fe(1A)–S(1A) 2.2505(19), Fe(1A)–S(3A) 2.2483(17); Fe(1A)–S(1A)–Fe(2A) 68.31(5), Fe(1A)–S(3A)–Fe(2A) 68.60(5).

larly to the ODT and SDT complexes, the bridgehead sulfur atoms in **3b** and **3d** are disordered (50%).

In contrast to the above-described NMR spectra for complexes **3b**–**d**, the ^1H and $^{13}C\{^1H\}$ NMR spectra of **6a**–**d** show that the R groups connected to the bridging carbon atoms (SCR_2SCR_2S) are chemically non-equivalent. For example, the ^1H NMR spectrum of **6a** contains the splitting pattern of an AA′BB′ system which was assigned to the protons of the two methylene groups, and the IR spectrum displays a characteristic vibration band at 1898 cm^{-1} assigned to the bridging CO ligands. Compound **6b** also shows two singlets attributed to two pairs of non-equivalent methyl groups. Similar observations were made for **6c** and **6d**. The desorption electron ionization (DEI) mass spectra for **6b**, **6c** and **6d** reveal the presence of $[M]^+$ ions at *m*/*z* 744, 800 and 824, respectively, and a stepwise fragmentation of eleven CO groups. Additionally, the IR spectroscopic measurements prove the presence of bridging CO ligands [ν(CO) = 1910 (for **6b**) and 1923, 1901 cm^{-1} (for **6c**)].

Complexes **6b**–**d** were characterised as tetranuclear iron clusters based on the X-ray diffraction analysis (Figure 4 and Figures S5 and S6 in the electronic supporting information). Compounds **6b**–**d** contain an $(OC)_3Fe(\mu\text{-}SCR_2SCR_2S\text{-}\mu)Fe$ fragment [**6b**: R = Me, **6c**: R = Et, **6d**: R = 1/2 $(CH_2)_5$] coordinated to an $Fe_2(CO)_6(\mu\text{-}CO)_2S$ unit which is likely to be formed in the reaction of $Fe_2(CO)_9$ with the sulfur originating from the decomposition of the in situ generated thiosulfinates (see below). The $Fe_2(CO)_6(\mu\text{-}CO)_2S$ moiety acts as a six-electron donor ligand that formally substitutes three CO ligands from the complex of type **3** to finally give an eight-coordinate Fe(2) atom. A similar cluster has been synthesised by the reaction of the sulfur with $Fe_3(CO)_{12}$ in 1-hexene to give $[Fe_4(CO)_{11}(\mu^3\text{-}S)(\mu\text{-}L)]$ (L = 1,2-hexylenedithiolate).[8a,b] In contrast to our results, very unusual triiron clusters with seven coordinated CO ligands were obtained when $[Fe_3(CO)_{12}]$ was treated with 1,2- and 1,3-dithioles in toluene at 70 °C.[8c] The Fe(1) and Fe(2) centres are μ^2-bridged by the alkyl-substituted SDT ligands and the Fe(2), Fe(3), Fe(4) and S(4) atoms form a tetrahedron. The Fe(1)–Fe(2) distances are about 0.04 Å longer than the corresponding bond lengths in **3b**–**d**, and the Fe(2)–Fe(3)/Fe(4) bond lengths in the tetrahedron are remarkably longer than the Fe(1)–Fe(2) distances [e.g. **6b**: 2.6419(9)/2.6365(10) Å].

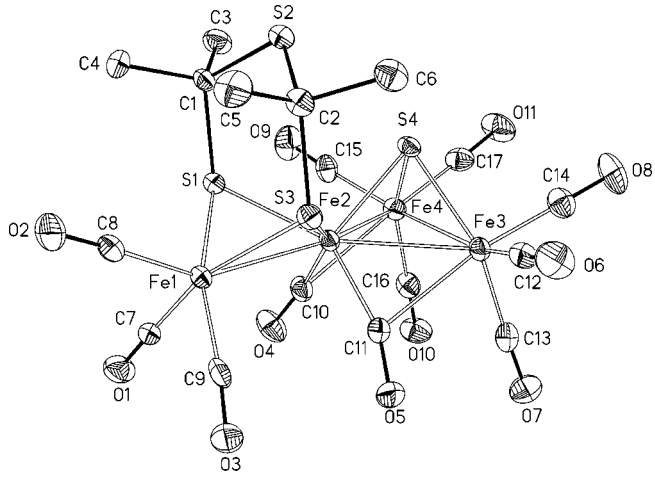

Figure 4. Structure of $[Fe_4(\mu\text{-}SCR_2SCR_2S\text{-}\mu)(CO)_9(\mu\text{-}CO)_2S]$ (**6b**; R = Me) showing thermal ellipsoids at the 50% probability level (hydrogen atoms have been omitted for clarity). Selected distances [Å] and angles [°]: Fe(1)–Fe(2) 2.5672(9), Fe(2)–Fe(3) 2.6419(9), Fe(2)–Fe(4) 2.6365(10), Fe(3)–Fe(4) 2.5855(10), Fe(1)–C(8) 1.804(6), Fe(1)–C(9) 1.806(6), Fe(2)–C(10) 1.813(6), Fe(2)–C(11) 1.827(6), Fe(3)–C(11) 2.381(5), Fe(1)–S(1) 2.2366, Fe(1)–S(3) 2.2329, Fe(2)–S(4) 2.2017(13); Fe(1)–S(1)–Fe(2) 69.65(4), Fe(1)–S(3)–Fe(2) 69.73(4), Fe(3)–Fe(2)–S(4) 52.72(4), Fe(4)–Fe(2)–S(4) 52.39(4), Fe(3)–Fe(2)–Fe(4) 58.66(3), Fe(3)–Fe(4)–Fe(2) 60.78(3).

Reaction of 1,2,4-Trithiolane 1e with $[Fe_2(CO)_9]$ (2)

The reaction of 1,2,4-trithiolane **1e** with three equivalents of **2** at room temperature in thf gave complexes **3e**, **4e** and **7** (Figures 5 and 6 and Figures S4 in the supporting information) which were separated by column chromatography (Scheme 4). Compound **4e** has already been isolated by Alper et al. from the reaction of adamantanethione with **2** in benzene.[3d] The single-crystal diffraction analysis of **3e** showed that the Fe–Fe distance [2.5525(13) Å] is about 0.045 Å longer than that in **3a** (Figure 5). The Fe–Fe distance in **3e** is very similar to that found in the reduced state diiron subsite of the enzyme structure (2.55 Å).[6a]

Due to the sterically demanding influence of the adamantyl substituents, the average Fe–S–Fe angle of 69.3° is slightly larger than that in **3a** (67.7°). The large C(1)–S(3)–C(11) angle of 111.4(3)° in **3e** differs significantly from that in complex **3a** [102.77(9)°].

Unlike the reactions of **1a**–**d** with **2**, the formation of a tetranuclear iron cluster similar to **6a**–**d** was not observed, although we were able to isolate complex **7**. The DEI mass

spectrum of **7** shows the [M$^+$] ion at *m*/*z* 586 and stepwise fragmentation of nine CO groups. This indicates that three $Fe(CO)_3$ moieties are coordinated to adamantanethione, a result which was also confirmed by X-ray structure analysis (Figure 6).

As a tentative mechanism we propose that the interaction of 1,2,4-trithiolanes **1a**–**e** with an $Fe_2(CO)_6$ complex fragment initially results in its insertion into the S–S bond to form complexes **3a**–**e**. But how can we explain the formation of complexes **4a**–**e**, **6a**–**d** and **7**? The insertion of iron carbonyl into the S–S bond, which results in the formation of **3** (Scheme 5, pathway a), competes with decomposition of the intermediate zwitterion to form **4** (Scheme 5, pathway b), which can be considered as a formal complex of $Fe_2(CO)_6$ with dithiirane, and the corresponding thioketone. In contrast to the enolisable aliphatic and cycloaliphatic thioketones, adamantanethione is a relatively stable compound,[9] which cannot undergo this undesired side reaction and is trapped in situ with the $Fe_3(CO)_9$ fragment to yield **7** (Scheme 5). Less stable aliphatic thioketones or products of their secondary transformations act as sulfur donors in the multistep reaction leading to clusters of type **6**.

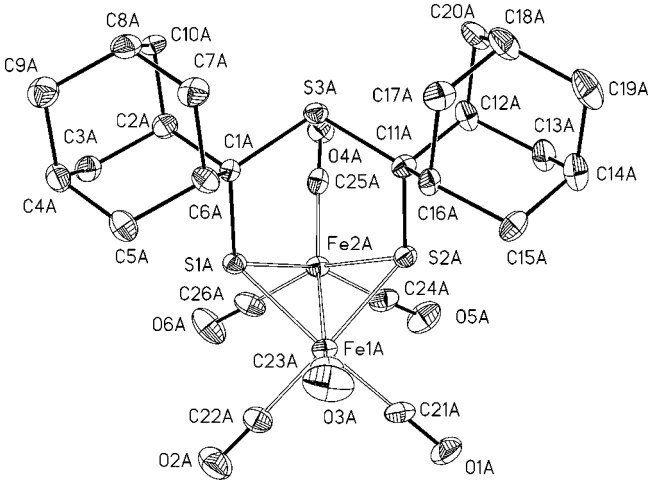

Figure 5. Structure of [Fe_2{SC(ad)SC(ad)S}$(CO)_6$] (ad = adamantyl) **3e** with thermal ellipsoids set at the 50% probability level (hydrogen atoms have been omitted for clarity). Selected distances [Å] and angles [°]: Fe(1A)–Fe(2A) 2.5525(13), Fe(1A)–C(A21) 1.803(8), Fe(A1)–C(A22) 1.785(8), Fe(A1)–C(A23) 1.807(8), Fe(1A)–S(1A) 2.247(2), Fe(1A)–S(2A) 2.2407(19); Fe(1A)–S(1A)–Fe(2A) 69.18(6), Fe(1A)–S(2A)–Fe(2A) 69.49(6).

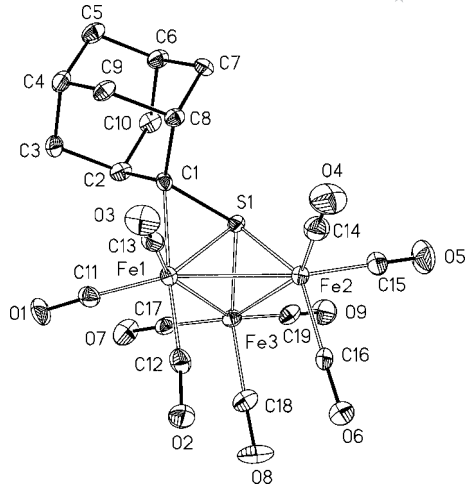

Figure 6. Structure of [Fe_3(ad)S$(CO)_9$] (**7**; ad = adamantyl) showing thermal ellipsoids at the 50% probability level (hydrogen atoms have been omitted for clarity). Selected distances [Å] and angles [°]: Fe(1)–Fe(2) 2.6256(11), Fe(2)–Fe(3) 2.6704(12), Fe(3)–Fe(1) 2.6272(12), Fe(1)–C(1) 2.122(6), Fe(1)–S(1) 2.2068(16), S(1)–C(1) 1.781(6); Fe(1)–C(1)–S(1) 68.2(2), Fe(1)–Fe(3)–Fe(2) 59.42(3), Fe(2)–Fe(1)–Fe(3) 61.11(3), Fe(1)–S(1)–Fe(2) 74.34(5), Fe(2)–S(1)–Fe(3) 77.28(6).

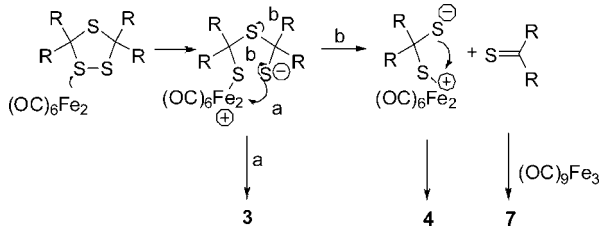

Scheme 5. Proposed mechanism for the formation of **3**, **4** and **7**.

In order to exclude the formation of complexes **4a**–**e** from **3a**–**e** we treated **3b** with an excess of **2** in thf at room temperature for 5 h. Complex **3b** does not react further under these conditions.

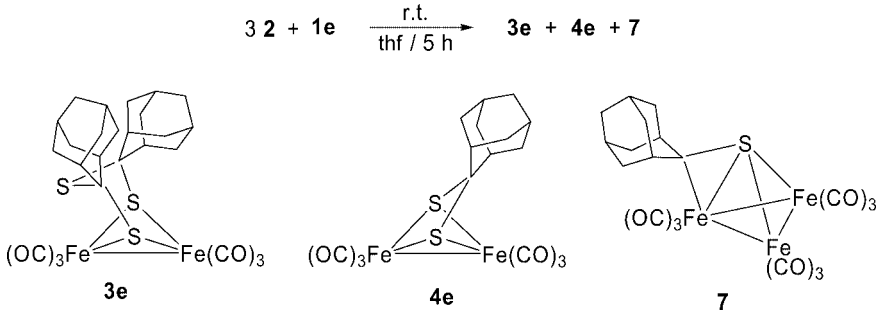

Scheme 4. Reaction of 1,2,4-trithiolane **1e** with [$Fe_2(CO)_9$].

Figure 6 shows that the adamantanethione molecule is bonded side-on to a three-iron triangle where Fe(1)–Fe(3) and S(1) form a tetrahedron. The C(1)–S(1) distance [1.781(6) Å] is significantly longer than that in a corresponding organic compound such as thiobenzoephenone due to this side-on coordination.[10]

Substitution Reaction of 3a with $(Et_4N)CN$

The displacement of one CO ligand with one equivalent of CN^- anion leads to the formation of complex **8**, which was successfully isolated from reaction mixture. This product is formed by the addition of $(Et_4N)CN$ to **3a**. The same reaction has been applied very recently to substitute two CO ligands by CN^- ions to yield $(Et_4N)_2[Fe_2(SDT)(CO)_4(CN)_2]$.[3c]

The ^1H NMR spectrum of **8** shows one broad singlet for the SCH_2S groups at $\delta = 2.59$ ppm, which is different to the corresponding resonances in $(Et_4N)_2[Fe_2(SDT)(CO)_4(CN)_2]$ ($\delta = 3.30$ ppm)[3c] and $(Et_4N)[Fe_2(ODT)(CO)_5(CN)]$ ($\delta = 4.09$ ppm).[7] Although both methylene groups in **8** and in $(Et_4N)[Fe_2(ODT)(CO)_5(CN)]$ are diastereotopic, the four protons appear as a broad singlet, which indicates a dynamic process in the complexes. The ESI mass spectrum of **8** reveals the anion at *m*/*z* 401.9 and the cation at *m*/*z* 130.2. All ν(CO) bands in the IR spectra are shifted, as expected, towards lower energies than in **3a** due to the negative charge of the complex. The isotopic pattern for the anion confirmed the postulated monocyanide complex **8** (see Figure S7 in the Supporting Information). The structure of **8** was confirmed by single-crystal X-ray diffraction (Figure 7), which unequivocally confirmed the formation of complex **8**. The Fe–Fe bond length [2.5240(12) Å] is slightly longer than that in **3a** and very similar to that in $(Et_4N)[Fe_2(PDT)(CN)(CO)_5]$ [2.5291(6) Å].[6b] In analogy to $(Et_4N)[Fe_2(PDT)(CN)(CO)_5]$, the five Fe–CO distances (1.77 Å) are shorter than the Fe–CN distance [1.940(6) Å]. In contrast to $(Et_4N)[Fe_2(ODT)(CN)(CO)_5]$, however, where the bridgehead oxygen atom is fixed completely opposite the Fe atom attached to the CN ligand, the bridgehead sulfur atom in complex **8** is orientated towards the Fe atom attached to the cyanide ligand.

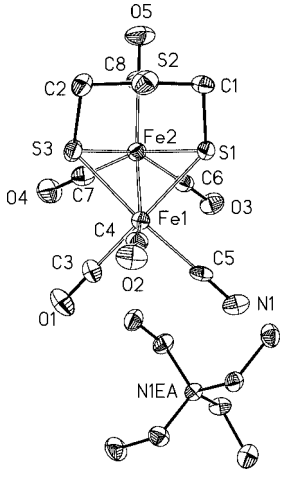

Figure 7. Structure of $(Et_4N)[Fe_2(SDT)(CN)(CO)_5]$ (**8**) showing thermal ellipsoids at the 50% probability level (hydrogen atoms have been omitted for clarity). Selected distances [Å] and angles [°]: Fe(1)–Fe(2) 2.5240(12), Fe(1)–C(3) 1.786(6), Fe(1)–C(4) 1.761(7), Fe(2)–C(5) 1.940(6), Fe(1)–S(1) 2.2488(16), Fe(1)–S(3) 2.2499(17); Fe(1)–S(1)–Fe(2) 67.93(5), Fe(1)–S(3)–Fe(2) 67.92(5).

Quantum Chemical Calculations

Geometry optimisation was performed at the RI-DFT and DFT levels with BP86 and B3LYP functionals and LANL2DZ, def-SV(P) basis sets using the TURBOMOLE[11–13] and Gaussian 03[14] software packages. The structure calculated for **9** (Figure 8), which differs from **6b** only in the substitution of the methyl groups for hydrogen, has main structural features that are very similar to those of **6b** and are in line with this complex being built up from an $Fe_2(CO)_6S$ (**10**; Figure 9) and an $Fe_2(CO)_5(SCH_2)_2S$ (**12**) unit. Complex **11** is the CO adduct of this latter fragment (Figure 10) and its structural data are similar to those of **3b**.

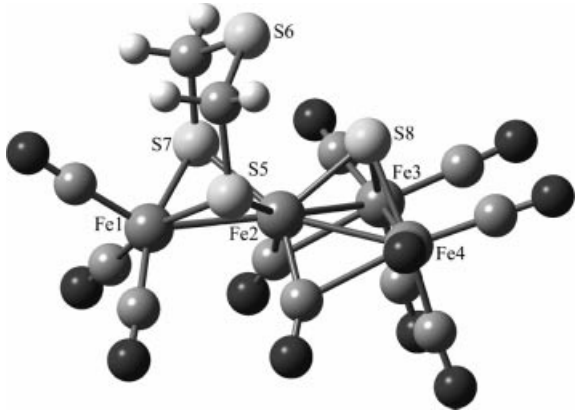

Figure 8. Structure of **9** obtained from the density functional calculations [BP86/def-SV(P)]. Selected distances [Å]: Fe(1)–Fe(2) 2.579, Fe(2)–Fe(3) 2.604, Fe(2)–Fe(4) 2.607, Fe(3)–Fe(4) 2.584, Fe(1)–C 1.775–1.799, Fe(2)–C 1.818, Fe(3)–C 1.785, 2.309, Fe(1)–S(5,7) 2.279, Fe(2)–S(5,7) 2.286, Fe(2)–S(8) 2.208, Fe(3)–S(8) 2.223.

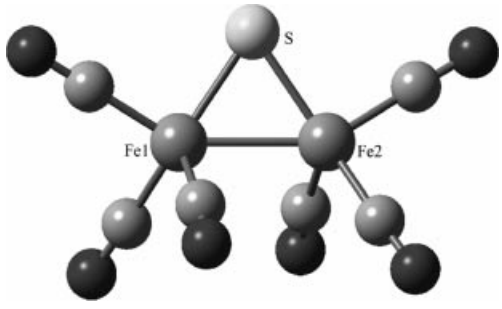

Figure 9. Structure of **10** obtained from the density functional calculations [BP86/def-SV(P)]. Selected distances [Å]: Fe(1)–Fe(2) 2.453, Fe–S 2.159, Fe–C 1.745–1.778.

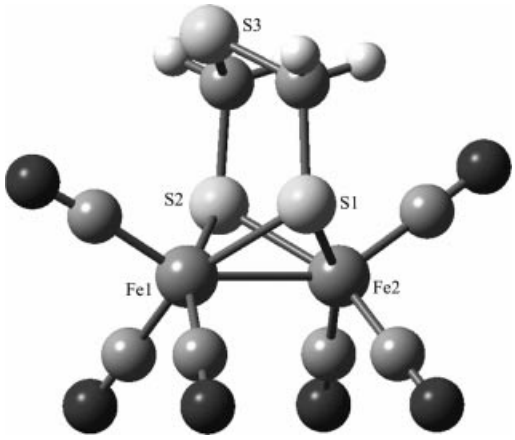

Figure 10. Structure of **11** obtained from the density functional calculations [BP86/def-SV(P)]. Selected distances [Å]: Fe(1)–Fe(2) 2.531, Fe–S 2.295–2.300, Fe–C 1.775–1.783.

Substitution of a CO ligand in **11** for **10** leaves the core of **11** essentially unaffected, whilst **10** is changed more drastically (the Fe–Fe and Fe–S distances are elongated by 0.1 Å). This is also shown by the shared electron numbers (SEN),[15] which indicate shorter Fe–Fe contacts in **10** ($SEN_{Fe–Fe}$ = 1.2) than in **11** ($SEN_{Fe–Fe}$ = 0.88). This is also the case for the Fe–S contacts [$SEN_{Fe–S}$ = 1.47 (**10**), 1.08 (**11**)].

Inspection of the frontier orbitals (Figure 11) shows that the **10** and **11** can be viewed in a first approximation as separate units that are linked mainly by an Fe–S interaction. The pseudo-bridging CO ligands on the Fe(2)–Fe(3,4) edges are only weakly bonded to Fe(3,4).

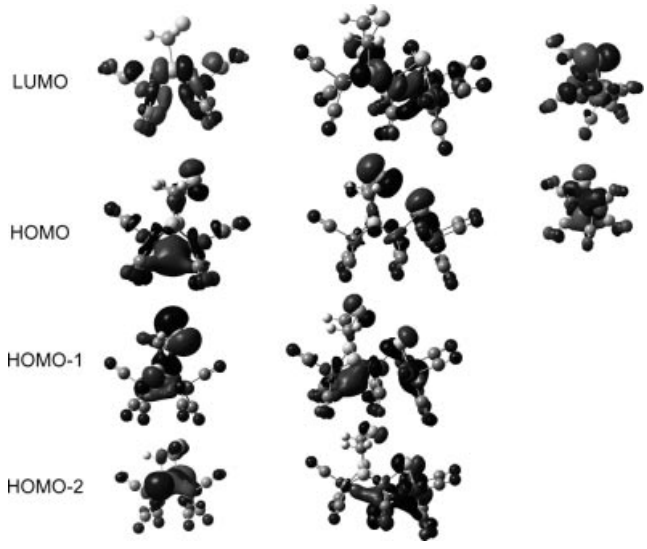

Figure 11. Kohn–Sham frontier orbitals for **9**–**11**.

An alternative description of **9** as a Fe_3S clusters with a $Fe(CO)_3$ ligand attached to two S atoms, as depicted in Scheme 3, might also be possible. Complex **12** would be balanced as a cluster with six skeletal electron pairs, which would fit a Wade-type[16,17] *nido* cluster isolobal with P_4. The results of the calculations on **9** and **11**, however, show that this interpretation is less valid.

Conclusions

We have shown that the 1,2,4-trithiolanes **1a**–**e** react with $[Fe_2(CO)_9]$ (**2**) by insertion into the S–S bond to provide novel mimics (**3a**–**e**) of [Fe-only] hydrogenase. We also succeeded in isolating the carbondithiolato (SCR_2S)-bridged diiron products **4a**–**e** and the tetranuclear clusters **6b**–**d** as side products. Interestingly, the reaction of **1e** with **2** yielded the adamantanethione complex **7** as well as **3e** and **4e**; no tetranuclear cluster of type **6** was observed. These reaction pathways can be explained by an interaction of the $Fe_2(CO)_6$ complex fragment with the disulfide moiety in the 1,2,4-trithiolanes **1a**–**e**, which induces ring opening. Reaction of the resulting zwitterionic intermediate competes with its decomposition to **4**, which can be considered as a formal complex of $Fe_2(CO)_6$ with dithiirane, and the corresponding thioketone. In the case of **7**, the eliminated adamantanethione, which is a relatively stable compound,[9] is trapped in situ by an $Fe_3(CO)_9$ fragment (Scheme 5). Less stable aliphatic thioketones or products of their secondary transformations act as sulfur donors in the multistep reaction leading to clusters of type **6**. Density functionl calculations have shown that tetrairon clusters of type **6** are built from two dinuclear subunits linked by iron–sulfur contacts.

Experimental Section

General: The ^1H and $^{13}C\{^1H\}$ NMR spectra were recorded with a Bruker DRX 200 or DRX 400 spectrometer using the solvent as reference. The 2D NMR measurements were done on the DRX 400 spectrometer. The mass spectra were recorded with a FINNIGAN MAT SSQ 710 instrument. The IR spectra were recorded with a Thermoelectron Nicolet AVATAR 30070 DTGS by using KBr pellets, with a Biorad FTF 25 in ATR cuvettetes when measuring neat substance and with a Perkin–Elmer 2000 FT-IR spectrometer when measuring solutions. 1,2,4-Trithiolane (**1a**), 3,3,5,5-tetramethyl-1,2,4-trithiolane (**1b**), 3,3,5,5-tetraethyl-1,2,4-trithiolane (**1c**), 3,3,5,5-bis(pentamethylene)-1,2,4-trithiolane (**1d**) and dispiro{tricyclo[3.3.1.1]decane-2,3′′-(1,2,4)-trithiolane-5′,2′-tricyclo[3.3.1.1]decane} (**1e**) were prepared according to literature protocols.[18–20] Elemental analyses were performed with LECO CHNS-932. Solvents and $[Fe_2(CO)_9]$ (**2**) were purchased from Sigma–Aldrich. Thf was dried with sodium/benzoephenone before use. Reported yields refer to the amount of purified products. Merck Silica gel 60 (0.015–0.040 mm) was used for column chromatography. TLC was performed on Merck TLC aluminium sheets (slica gel 60 F_{254}).

Preparation of Complexes 3a–e, 4a–e, 6a–d and 7. General Procedure: Nonacarbonyldiiron (**2**; 4.5 mmol) and 1,2,4-trithiolane **1a**–**e** (1.5 mmol) were dissolved in thf (20 mL) and stirred at room temperature for five hours under argon. The light-orange solution turned deep red and a brown solid (mixture of inorganic iron sulfides) precipitated. The solvent was removed under reduced pressure and the crude product was purified by column chromatography using hexane as eluent. A yellow fraction representing the

side products **4a**–**e**, the orange main fraction containing complexes **3a**–**e**, and the third, red-brown and brown fractions containing **6a** and **6b**–**d** and **7**, respectively, were collected and the solvent removed in vacuo. The products were obtained as red-orange (for **3a**–**e** and **4a**–**e**), dark-red (for **6a**) or brown solids (for **6b**–**d** and **7**).

Crystals suitable for X-ray diffraction analysis were obtained by slow evaporation of hexane into a concentrated pentane solution at 0 °C (for **3a**–**e**). Products **3a**–**e**, **4a**–**e**, **6b**–**d** and **7** were crystallised from a solution of hexane at –25 °C.

[Fe$_2$(SDT)(CO)$_6$] (3a):[3] R_f = 0.5 (hexane): Yield 234 mg (0.58 mmol, 38.6%). $C_8H_4Fe_2O_6S_3$ (403.79): calcd. C 23.78, H 0.99, S 23.81; found C 23.81, H 1.26, S 23.48. ^{1}H NMR (200 MHz, $CDCl_3$, 25 °C): δ = 3.21 (s, 4 H, CH_2) ppm. ^{13}C{^{1}H} NMR (100 MHz, $CDCl_3$): δ = 27.7 (*C*H$_2$), 206.8 (*C*O) ppm. FT-IR (KBr disc): $\tilde{\nu}$ = 2075 (s), 2027 (s), 1999 [vs (νCO, terminal)] cm^{-1}. MS (DEI, 70 eV): *m*/*z* 404 (16) [M$^+$], 376 (100) [M$^+$ – CO], 348 (70) [M$^+$ – 2CO], 320 (46) [M$^+$ – 3CO], 292 (17) [M$^+$ – 4CO], 264 (42) [M$^+$ – 5CO], 236 (58) [M$^+$ – 6CO], 208 (58) [M$^+$ – 5CO – Fe], 176 (26) [M$^+$ – 5CO – Fe – S], 144 (68) [M$^+$ – 5CO – Fe – 2S], 122 (12) [M$^+$ – 5CO – Fe – 3S], 78 (8) [CH_2S_2], 56 (26), 45 (12) [CHS].

[Fe$_2${SC(CH$_3$)$_2$SC(CH$_3$)$_2$S}(CO)$_6$] (3b): R_f = 0.49 (hexane). Yield 251.8 mg (0.548 mmol, 36.5%). $C_{12}H_{12}Fe_2O_6S_3$ (460.11): calcd. C 31.33, H 2.63, S 20.91; found C 31.24, H 2.89, S 20.72. ^{1}H NMR (200 MHz, $CDCl_3$, 25 °C): δ = 1.61 (s, 12 H, CH_3) ppm. ^{13}C{^{1}H} NMR (100 MHz, $CDCl_3$, 25 °C): δ = 35.3 (*C*H$_3$), 46.0 (C_q), 207.3 (*C*O) ppm. FT-IR (KBr disc): $\tilde{\nu}$ = 2073 (s), 2029 (s), 2002 (vs), 1970 [s (νCO, terminal)] cm^{-1}. MS (DEI, 70 eV): *m*/*z* (%) 460 (2) [M$^+$], 432 (30) [M$^+$ – CO], 404 (38) [M$^+$ – 2CO], 376 (36) [M$^+$ – 3CO], 348 (26) [M$^+$ – 4CO], 320 (60) [M$^+$ – 5CO], 292 (56) [M$^+$ – 6CO].

[Fe$_2${SC(CH$_2$CH$_3$)$_2$SC(CH$_2$CH$_3$)$_2$S}(CO)$_6$] (3c): R_f = 0.48 (hexane). Yield 309.6 mg (0.6 mmol, 40%). $C_{16}H_{20}Fe_2O_6S_3$ (516.21): calcd. C 37.23, H 3.91, S 18.63; found C 37.21, H 3.86, S 18.64. ^{1}H NMR (200 MHz, $CDCl_3$, 25 °C): δ = 0.98 (t, ^3J = 7.2 Hz, 12 H, CH_3), 1.76 (q, ^3J = 7.6 Hz, 4 H, CH_2), 1.77 (q, ^3J = 7.6 Hz, 4 H, CH_2) ppm. ^{13}C{^{1}H} NMR (100 MHz, $CDCl_3$, 25 °C): δ = 9.3 (*C*H$_3$), 23.4 (*C*H$_2$), 54.3 (C_q), 207.5 (*C*O) ppm. FT-IR (KBr disc): $\tilde{\nu}$ = 2073 (s), 2028 (s), 2013 (s), 1985 (s), 1973 [s (νCO, terminal)] cm^{-1}. MS (DEI, 70 eV): *m*/*z* (%) 516 (29) [M$^+$], 488 (100) [M$^+$ – CO], 460 (67) [M$^+$ – 2CO], 432 (86) [M$^+$ – 3CO], 404 (52) [M$^+$ – 4CO], 376 (84) [M$^+$ – 5CO], 248 (63) [M$^+$ – 6CO].

[Fe$_2${SC[(CH$_2$)$_5$]SC[(CH$_2$)$_5$]S}(CO)$_6$] (3d): R_f = 0.57 (hexane). Yield 332.1 mg (0.615 mmol, 41%). $C_{18}H_{20}Fe_2O_6S_3$ (540.23): calcd. C 40.02, H 3.73, S 17.81; found C 40.04, H 3.90, S 17.59. ^{1}H NMR (200 MHz, $CDCl_3$, 25 °C): δ = 1.84 (m, 8 H, CCH_2CH$_2$), 1.65 (m, 8 H, CCH$_2$CH_2), 1.47 and 1.33 (m, 4 H, CCH$_2$CH$_2$CH_2) ppm. ^{13}C{^{1}H} NMR (100 MHz, $CDCl_3$): δ = 22.8 (CCH$_2$*C*H$_2$), 25.2 (CCH$_2$CH$_2$*C*H$_2$), 43.2 (C*C*H$_2$CH$_2$), 50.8 (C_q), 207.6 (*C*O) ppm. FT-IR (KBr disc): $\tilde{\nu}$ = 2072 (s), 2035 (vs), 2014 (s), 1985 [s (νCO, terminal)] cm^{-1}. MS (DEI, 70 eV): *m*/*z* (%) 540 (3) [M$^+$], 512 (34) [M$^+$ – CO], 484 (30) [M$^+$ – 2CO], 456 (44) [M$^+$ – 3CO], 428 (40) [M$^+$ – 4CO], 400 (64) [M$^+$ – 5CO], 372 (100) [M$^+$ – 6CO].

[Fe$_t$SC(ad)SC(ad)S}(CO)$_6$] (3e): R_f = 0.6 (hexane). Yield 328.4 mg (0.51 mmol, 34%). $C_{26}H_{28}Fe_2O_6S_3$ (644.38): calcd. C 48.46, H 4.38, S 14.90; found C 48.18, H 4.37, S 14.39. ^{1}H NMR (200 MHz, $CDCl_3$): δ = 1.41–1.69 (m, 16 H), 1.88 (s, 4 H), 2.52 (m, 4 H), 2.72 (m, 4 H) ppm. ^{13}C{^{1}H} NMR (100 MHz, $CDCl_3$): δ = 26.7, 26.9 (4*C*H), 33.6, 34.4 (2 and 4 *C*H$_2$), 38.6 (4 *C*H), 41.6 (4 *C*H$_2$), 60.2 (2 C_q), 207.5 (*C*O) ppm. FT-IR (KBr disc): $\tilde{\nu}$ = 2070 (s), 2033 (s), 1994 (s), 1980 [s (νCO, terminal)] cm^{-1}. MS (DEI, 70 eV): *m*/*z* (%) 644 (2) [M$^+$], 616 (6) [M$^+$ – CO], 588 (4) [M$^+$ – 2CO], 560 (26) [M$^+$ – 3CO], 532 (28) [M$^+$ – 4CO], 504 (44) [M$^+$ – 5CO], 476 (100) [M$^+$ – 6CO].

[Fe$_2${SC(CH$_2$)S}(CO)$_6$] (4a):[4] R_f = 0.52 (hexane). This product obtained by column chromatography was partially contaminated with **5**,[5] therefore the corresponding yield could not be determined exactly. Yield approx. 46.5 mg (approx. 0.13 mmol, 8.6%). ^{1}H NMR (200 MHz, $CDCl_3$, 25 °C): δ = 4.60 (s, 2 H, CH_2) ppm.

[Fe$_2${SC(CH$_3$)$_2$S}(CO)$_6$] (4b): R_f = 0.54 (hexane). Yield 85.7 mg (0.22 mmol, 14.8%). HR-MS (ESI) calcd. for $C_9H_6Fe_2O_6S_3$: 385.8305; found 385.8305. ^{1}H NMR (200 MHz, $CDCl_3$, 25 °C): δ = 1.76 (s, 4 H, CH_2) ppm. ^{13}C{^{1}H} NMR (100 MHz, $CDCl_3$): δ = 40.9 (*C*H$_3$), 83.4 (C_q), 208.6 (*C*O) ppm. FT-IR (KBr disc): $\tilde{\nu}$ = 2072 (s), 2025 (s), 2006 (s), 1983 (m), 1963 [m (νCO, terminal)] cm^{-1}. MS (DEI, 70 eV): *m*/*z* (%) 386 (26) [M$^+$], 358 (16) [M$^+$ – CO], 330 (20) [M$^+$ – 2CO], 302 (14) [M$^+$ – 3CO], 274 (24) [M$^+$ – 4CO], 246 (32) [M$^+$ – 5CO], 218 (74) [M$^+$ – 6CO], 176 (100) [Fe_2S_2].

[Fe$_2${SC(CH$_2$CH$_3$)$_2$S}(CO)$_6$] (4c): R_f = 0.55 (hexane). Yield 40.4 mg (0.1 mmol, 6.5%). ^{1}H NMR (200 MHz, $CDCl_3$, 25 °C): δ = 0.79 (t, ^3J = 7.4 Hz, 12 H, CH_3), 2.05 (q, ^3J = 7.4 Hz, 8 H, CH_2) ppm. ^{13}C{^{1}H} NMR (100 MHz, $CDCl_3$, 25 °C): δ = 7.1 (*C*H$_3$), 40.6 (*C*H$_2$), 93.3 (C_q), 208.6 (*C*O) ppm. MS (DEI, 70 eV): *m*/*z* (%) 414 (100) [M$^+$], 386 (82) [M$^+$ – CO], 358 (61) [M$^+$ – 2CO], 330 (67) [M$^+$ – 3CO], 302 (37) [M$^+$ – 4CO], 274 (54) [M$^+$ – 5CO], 246 (21) [M$^+$ – 6CO].

[Fe$_2${SC[(CH$_2$)$_5$]S}(CO)$_6$] (4d): R_f = 0.73 (hexane). Yield 56.9 mg (0.13 mmol, 8.9%). $C_{12}H_{10}Fe_2O_6S_2$ (426.02): calcd. C 33.83, H 2.37, S 15.05; found C 33.89, H 2.64, S 15.33. ^{1}H NMR (200 MHz, $CDCl_3$, 25 °C): δ = 2.09 (m, 4 H, CCH_2CH$_2$), 1.43 (m, 4 H, CCH$_2$CH_2), 1.38 (m, 2 H, CCH$_2$CH$_2$CH_2) ppm. ^{13}C{^{1}H} NMR (100 MHz, $CDCl_3$): δ = 22.0 (CCH$_2$*C*H$_2$), 26.1 (CCH$_2$CH$_2$*C*H$_2$), 49.8 (C*C*H$_2$CH$_2$), 89.9 (C_q), 208.6 (*C*O) ppm. FT-IR (KBr disc): $\tilde{\nu}$ = 2074 (s), 2032 (s), 2002 (s), 1969 [s (νCO, terminal)] cm^{-1}. MS (DEI, 70 eV): *m*/*z* (%) 426 (100) [M$^+$], 398 (82) [M$^+$ – CO], 370 (64) [M$^+$ – 2CO], 342 (47) [M$^+$ – 3CO], 314 (43) [M$^+$ – 4CO], 286 (25) [M$^+$ – 5CO], 258 (60) [M$^+$ – 6CO].

[Fe$_2${SC(ad)S}(CO)$_6$] (4e): R_f = 0.62 (hexane). Yield 117.6 mg (0.25 mmol, 16.4%). $C_{16}H_{14}Fe_2O_6S_2$ (478.1): calcd. C 40.19, H 2.95, S 13.41; found C 40.21, H 2.92, S 13.18. ^{1}H NMR (200 MHz, $CDCl_3$, 25 °C): δ = 2.57 (br. s, 2 H, 2C*H*), 1.87 and 1.56 (d, ^2J = 12.4 Hz, 8 H, 4CH_2), 1.77 (br. s, 2 H, 2C*H*), 1.67 (br. s, 2 H, CH_2) ppm. ^{13}C{^{1}H} NMR (100 MHz, $CDCl_3$): δ = 27.6 (2*C*H), 31.9 (4 *C*H$_2$), 37.0 (*C*H$_2$), 49.1 (2 *C*H), 98.3 (C_q), 208.6 (CO) ppm. FT-IR (KBr disc): $\tilde{\nu}$ = 2070 (s), 2026 (s), 2000 (s), 1983 [s (νCO, terminal)] cm^{-1}. MS (DEI, 70 eV): *m*/*z* (%) 478 (54) [M$^+$], 450 (30) [M$^+$ – CO], 422 (24) [M$^+$ – 2CO], 394 (28) [M$^+$ – 3CO], 366 (47) [M$^+$ – 4CO], 338 (35) [M$^+$ – 5CO], 310 (100) [M$^+$ – 6CO].

[Fe$_4$(μ-SCH$_2$SCH$_2$S-μ)(CO)$_9$(μ-CO)$_2$S] (6a): Yield 31 mg (0.045 mmol, 3%). ^{1}H NMR (200 MHz, $CDCl_3$, 25 °C): δ = 3.1 (m, AA′BB′ spin system, 4 H, 2CH_2) ppm. ^{13}C{^{1}H} NMR (100 MHz, $CDCl_3$): δ = 26.8 (*C*H$_2$), 26.9 (*C*H$_2$), 203.5 and 206.8 (*C*O) ppm. FT-IR (KBr disc): $\tilde{\nu}$ = 2068 (s), 2034 (s), 1997 (s), 1975 [s (νCO, terminal)], 1898 [m (ν(μ^2-CO)] cm^{-1}.

[Fe$_4$(μ-SCMe$_2$SCMe$_2$S-μ)(CO)$_9$(μ-CO)$_2$S] (6b): Yield 24.6 mg (0.033 mmol, 2.2%). $C_{17}H_{12}Fe_4O_{11}S_4$ (743.91): calcd. C 27.45, H 1.63, S 17.24; found C 27.53, H 2.15, S 16.90. ^{1}H NMR (200 MHz, $CDCl_3$, 25 °C): δ = 1.6 (s, 6 H, CH_3), 1.87 (s, 6 H, CH_3) ppm. ^{13}C{^{1}H} NMR (100 MHz, $CDCl_3$): δ = 34.1 and 35.0 (*C*H$_3$), 49.4 (C_q) ppm. FT-IR (ATR cuvette): $\tilde{\nu}$ = 2079 (w), 2056 (m), 2026 (m), 2009 (s), 1978 [s (νCO, terminal)], 1923, 1910 [ν(μ^2-CO)] cm^{-1}. MS (DEI, 70 eV): *m*/*z* (%) 744 (0.1) [M$^+$], 716 (1) [M$^+$ – CO], 688 (1.2) [M$^+$ – 2CO], 660 (2.7) [M$^+$ – 3CO], 632 (0.4) [M$^+$ – 4CO], 604 (3.2)

[M⁺ – 5CO], 576 (4.4) [M⁺ – 6CO], 548 (3.7) [M⁺ – 7CO], 520 (100) [M⁺ – 8CO], 492 (5) [M⁺ – 9CO].

[Fe_4(μ-$SCEt_2SCEt_2S$-μ)(CO)$_9$(μ-$CO)_2$S] (6c): Yield 24 mg (0.03 mmol, 2%). ^{1}H NMR (400 MHz, $CDCl_3$, 25 °C): δ = 0.95 (m, 12 H, CH_3), 1.73 (m, 4 H, CH_2), 1.87 and 2.21 (m, 4 H, CH_2) ppm. ^{13}C{^{1}H} NMR (100 MHz, $CDCl_3$): δ = 8.9 and 9.7 (*C*H_3), 33.2 and 34.4 (*C*H_2), 57.7 (C_q) ppm. FT-IR (KBr disc): $\tilde{\nu}$ = 2084 (m), 2058 (s), 2015 (s), 1993 (s), 1969 [m (νCO, terminal)], 1924, 1902 [ν(μ²-CO)] cm^{-1}. MS (DEI, 70 eV): *m*/*z* (%) 800 (0.1) [M⁺], 772 (0.3) [M⁺ – CO], 744 (0.9) [M⁺ – 2CO], 716 (4.6) [M⁺ – 3CO], 688 (0.1) [M⁺ – 4CO], 660 (3) [M⁺ – 5CO], 632 (3.9) [M⁺ – 6CO], 604 (2.3) [M⁺ – 7CO], 576 (9.2) [M⁺ – 8CO], 548 (2.3) [M⁺ – 9CO], 520 (4.6) [M⁺ – 10CO], 492 (17.7) [M⁺ – 11CO].

[Fe_4(μ-SCR_2SCR_2S-μ)(CO)$_9$(μ-$CO)_2$S] (6d) [R = 1/2(CH_2)$_5$]: Yield 28.4 mg (0.035 mmol, 2.3%). $C_{23}H_{20}Fe_4O_{11}S_4$ (824.04): calcd. C 33.52, H 2.45, S 15.56; found C 33.34, H 2.94, S 14.67. ^{1}H NMR (400 MHz, $CDCl_3$, 25 °C): δ = 1.25 and 1.51 (m, 4 H, $CCH_2CH_2CH_2$), 1.66 (m, 8 H, CCH_2CH_2), 1.84 and 2.37 (m, 4 H, CCH_2CH_2), 1.84 and 1.89 (m, 4 H, CCH_2CH_2) ppm. ^{13}C{^{1}H} NMR (100 MHz, $CDCl_3$): δ = 23.2 and 23.3 (CCH_2CH_2), 25.0 ($CCH_2CH_2CH_2$), 41.6 and 43.6 (CCH_2CH_2), 54.1 (C_q), 222.8 (*C*O) ppm. FT-IR (ATR cuvette): $\tilde{\nu}$ = 2077 (m), 2054 (m), 2028 (m), 2005 (s), 1969 [m (νCO, terminal)], 1913, 1897 [ν(μ²-CO)] cm^{-1}. MS (DEI, 70 eV): *m*/*z* (%) 824 (0.1) [M⁺], 796 (0.2) [M⁺ – CO], 768 (0.4) [M⁺ – 2CO], 740 (1) [M⁺ – 3CO], 712 (0.1) [M⁺ – 4CO], 684 (0.1) [M⁺ – 5CO], 656 (0.1) [M⁺ – 6CO], 628 (0.1) [M⁺ – 7CO], 600 (0.4) [M⁺ – 8CO], 572 (0.1) [M⁺ – 9CO], 544 (0.3) [M⁺ – 10CO], 516 (1) [M⁺ – 11CO].

[Fe_3(CO)$_9$S(ad)] (7; ad = adamantyl): Yield 7 mg (4.3%). ^{1}H NMR (400 MHz, $CDCl_3$, 25 °C): δ = 2.00–2.40 (m, 14 H) ppm. ^{13}C{^{1}H} NMR (100 MHz, $CDCl_3$): δ = 37.7, 37.6, 49.9, 56.8 (4CH and 5*C*H_2), 211.3 (*C*O) ppm; C_q not observed. FT-IR (ATR cuvette): $\tilde{\nu}$ = 2071 (m), 2005 (s), 1978 (s), 1965 [m (νCO, terminal)] cm^{-1}. MS (DEI, 70 eV): *m*/*z* (%) 586 (12) [M⁺], 558 (13) [M⁺ – CO], 530 (5) [M⁺ – 2CO], 502 (30) [M⁺ – 3CO], 474 (46) [M⁺ – 4CO], 446 (57) [M⁺ – 5CO], 418 (98) [M⁺ – 6CO], 390 (100) [M⁺ – 7CO], 362 (65) [M⁺ – 8CO], 334 (92) [M⁺ – 9CO]

Preparation of the Monocyanide Complex (Et_4N)[Fe_2(SDT)(CO)$_5$-(CN)] (8): A solution of **3a** (100 mg, 0.25 mmol) in MeCN (15 mL) at 0 °C was treated with a solution of Et_4NCN (80 mg, 0.50 mmol) in MeCN (15 mL). After warming the reaction mixture to room temperature, it was stirred for an additional 1.5 h. The solvent was then removed in vacuo and the residue washed thoroughly with diethyl ether and hexane. The washed residue was again evaporated to dryness to give a red solid. Single crystals suitable for X-ray diffraction analysis were obtained by diffusion of pentane into its MeCN solution. Yield 120 mg (90%). ^{1}H NMR (200 MHz, CD_3CN): δ = 3.18 (br. s, 8 H, CH_2CH_3), 2.43 (br. s, 4 H, SCH_2), 1.10 (br. s, 12 H, CH_2CH_3) ppm. ^{13}C{^{1}H} NMR (100 MHz, CD_3CN): δ = 8.0 (CH_2CH_3), 27.3 (SCH_2), 53.3 (CH_2CH_3), 150.7 (*C*N), 219.7 (*C*O) ppm. FT-IR (thf solution): $\tilde{\nu}$ = 2052 [s (νCN)], 2033 (s), 1981 (s), 1953 (m), 1921 [w (νCO, terminal)] cm^{-1}. MS (ESI pos., 70 eV): *m*/*z* (%) 130.2 (100) [M⁺, $C_8H_{20}N$]. MS (ESI neg., 70 eV): *m*/*z* (%) 401.9 (100) [M⁻, $C_8H_4Fe_2NO_5S_3$].

Supporting Information (see also the footnote on the first page of this article): Figures S1, S3 and S4 display the X-ray structures of compounds **4b**, **4d** and **4e**. The structure of **4c** is available as Figure S2. Figures S5 and S6 present the X-ray structures of **6c** and **6d**, respectively. Figure S7 shows the experimental and theoretical isotopic pattern of **8**⁻ (anion of **8**).

X-ray Structure Determination of 3b, 3c, 3d, 3e, 4b, 4c, 4d, 4e, 6b, 6c, 6d, 7 and 8:[21] Intensity data were collected with a Nonius Kappa CCD diffractometer using graphite-monochromated Mo-K_α radiation. Data were corrected for Lorentz polarisation, but not for absorption effects.[22,23] Crystallographic data as well as structure solution and refinement details are summarised in Tables 1 and 2.

The structures were solved by direct methods (SHELXS[24]) and refined by full-matrix least-squares techniques against F_o^2 (SHELXL-97[25]). The hydrogen atoms were included at calculated

Table 1. Crystal data and refinement details for the X-ray structure determinations.

	3b	**3c**	**3d**	**3e**	**4b**	**4c**	**4d**
Formula	$C_{12}H_{12}Fe_2O_6S_3$	$C_{16}H_{20}Fe_2O_6S_3$	$C_{18}H_{20}Fe_2O_6S_3$	$C_{26}H_{28}Fe_2O_6S_3$	$C_9H_6Fe_2O_6S_2$	$C_{11}H_{10}Fe_2O_6S_2$	$C_{12}H_{10}Fe_2O_6S_2$
Fw [g mol^{-1}]	460.10	516.20	540.22	644.36	385.96	414.01	426.02
T [°C]	–90(2)	–90(2)	–90(2)	–90(2)	–90(2)	–90(2)	–90(2)
Crystal system	triclinic	monoclinic	triclinic	monoclinic	triclinic	monoclinic	triclinic
Space group	$P\bar{1}$	$P2_1/c$	$P\bar{1}$	$C2/c$	$P\bar{1}$	$C2/c$	$P\bar{1}$
a [Å]	8.1108(3)	8.9271(2)	9.7862(9)	30.2126(11)	8.6954(3)	31.268(2)	11.6020(4)
b [Å]	10.3222(4)	11.0165(3)	14.9104(18)	10.0703(4)	11.5723(4)	18.3625(13)	12.7499(5)
c [Å]	11.1169(4)	21.7868(4)	16.824(2)	47.6223(17)	14.9455(5)	43.754(4)	17.2305(4)
α [°]	76.155(2)	90	64.218(5)	90	110.606(2)	90	105.944(2)
β [°]	81.608(2)	96.496(1)	83.966(8)	100.493(1)	94.740(2)	95.507(3)	101.834(2)
γ [°]	82.637(2)	90	81.145(8)	90	97.143(2)	90	93.938(2)
V [Å^3]	889.78(6)	2128.88(8)	2182.1(4)	14246.8(9)	1383.77(8)	25006(3)	2377.41(14)
Z	2	4	4	20	4	64	6
ρ [g cm^{-3}]	1.717	1.611	1.644	1.502	1.853	1.760	1.785
μ [cm^{-1}]	20.04	16.85	16.48	12.76	24.13	21.43	21.16
Measured data	6370	14854	12537	32291	9476	35222	16087
Data with $I > 2\sigma(I)$	3486	4005	5206	9270	3803	10112	7799
Unique data	4037	4866	9001	14543	6204	21331	10540
wR_2 (all data, on F^2)[a]	0.1069	0.0710	0.1611	0.2018	0.2849		0.0884
R_1 [$I > 2\sigma(I)$][a]	0.0411	0.0279	0.0650	0.0709	0.0834		0.0355
s[b]	1.012	1.010	1.032	1.024	1.050		0.980
Resid. dens. [e Å^{-3}]	1.577/–1.256	0.279/–0.400	0.530/–0.774	0.970/–0.572	1.839/–0.746		0.569/–0.536
Absorption correction	none	none	none	none	none	none	none

[a] $R_1 = (\Sigma||F_o| - |F_c||)/\Sigma|F_o||$, $wR_2 = \{\Sigma[w(F_o^2 - F_c^2)^2]/\Sigma[w(F_o^2)^2]\}^{1/2}$ with $w^{-1} = \sigma^2(F_o^2) + (aP)^2$. [b] $s = \{\Sigma[w(F_o^2 - F_c^2)^2]/(N_o - N_p)\}^{1/2}$.

Table 2. Crystal data and refinement details for the X-ray structure determinations.

	4e	**6b**	**6c**	**6d**	**7**	**8**
Formula	$C_{16}H_{14}Fe_2O_6S_2$	$C_{17}H_{12}Fe_4O_{11}S_4$	$C_{21}H_{20}Fe_4O_{11}S_4$	$C_{23}H_{20}Fe_4O_{11}S_4$	$C_{19}H_{14}Fe_3O_9S$	$C_8H_4Fe_2NO_5S_3{\cdot}C_8H_{20}N$
Fw [g mol^{-1}]	478.09	743.91	800.01	824.03	585.91	532.25
T [°C]	–90(2)	–90(2)	–90(2)	–90(2)	–90(2)	–90(2)
Crystal system	monoclinic	triclinic	triclinic	triclinic	monoclinic	monoclinic
Space group	$P2_1/n$	$P\bar{1}$	$P\bar{1}$	$P\bar{1}$	$P2/c$	$P2_1$
a [Å]	9.3431(3)	9.9870(6)	9.8115(5)	11.3477(13)	13.1719(5)	7.4131(6)
b [Å]	14.0459(3)	11.4368(6)	11.7948(5)	11.9251(17)	7.9576(2)	12.6401(13)
c [Å]	14.5478(5)	12.9150(8)	13.0075(6)	12.4537(18)	20.7565(8)	12.1092(10)
α [°]	90	73.088(3)	105.078(3)	83.751(6)	90	90
β [°]	106.955(2)	82.212(3)	94.819(2)	73.305(8)	99.768(2)	101.290(6)
γ [°]	90	64.417(3)	93.969(3)	66.080(8)	90	90
V [Å^3]	1826.16(9)	1272.90(13)	1441.82(12)	1475.5(3)	2144.09(13)	1112.70(17)
Z	4	2	2	2	4	2
ρ [g cm^{-3}]	1.739	1.941	1.843	1.855	1.815	1.589
μ [cm^{-1}]	18.47	26.16	23.16	22.67	21.49	16.13
Measured data	12112	9105	9971	9388	14777	7420
Data with $I > 2\sigma(I)$	3526	3897	4765	4034	3853	3212
Unique data	4151	5765	6538	6474	4897	4771
wR_2 (all data, on F^2)[a]	0.0679	0.1356	0.1015	0.1831	0.1613	0.1014
R_1 [$I > 2\sigma(I)$][a]	0.0265	0.0515	0.0433	0.0658	0.0635	0.0517
s[b]	1.016	0.986	1.027	1.054	1.136	0.955
Resid. dens. [e Å^{-3}]	0.343/–0.525	1.139/–0.723	0.681/–0.531	0.830/–1.129	1.431/–0.696	0.442/–0.471
Flack parameter	–	–	–	–	–	–0.01(2)
Absorption correction	none	none	none	none	none	none

[a] $R_1 = (\Sigma||F_o| - |F_c||/\Sigma|F_o|$, $wR_2 = \{\Sigma[w(F_o^2 - F_c^2)^2]/\Sigma[w(F_o^2)^2]\}^{1/2}$ with $w^{-1} = \sigma^2(F_o^2) + (aP)^2$. [b] $s = \{\Sigma[w(F_o^2 - F_c^2)^2]/(N_o - N_p)\}^{1/2}$.

positions with fixed thermal parameters. All non-hydrogen atoms except for the disordered part of molecules were refined anisotropically.[25] The quality of the data of compound **4c** was poor therefore we will only publish the conformation of the molecule and the crystallographic data. The data have no been deposited in the Cambridge Crystallographic Data Centre.

Acknowledgments

Financial support for this work was provided by the Freistaat Thüringen (Landesgraduiertenstipendium for J. W.). We are grateful to Ulf-Peter Apfel for experimental assistance.

[1] a) S. M. Aucott, H. L. Milton, S. D. Robertson, A. M. Z. Slawin, G. B. Walker, J. D. Woollins, *Chem. Eur. J.* **2004**, *10*, 1666–1676; b) S. M. Aucott, P. Kilian, S. D. Robertson, A. M. Z. Slawin, J. D. Woollins, *Chem. Eur. J.* **2006**, *12*, 895–902; c) S. M. Aucott, P. Kilian, H. L. Milton, S. D. Robertson, A. M. Z. Slawin, J. D. Woollins, *Inorg. Chem.* **2005**, *44*, 2710–2718; d) A. Ishii, M. Saito, M. Murata, J. Nakayama, *Eur. J. Org. Chem.* **2002**, 979–982; e) A. Ishii, T. Kawai, M. Noji, J. Nakayama, *Tetrahedron Lett.* **2005**, *61*, 6693–6699; f) A. Ishii, M. Murata, H. Oshida, K. Matsumoto, J. Nakayama, *Eur. J. Inorg. Chem.* **2003**, 3716–3721.

[2] W. Weigand, S. Bräutigam, G. Mloston, *Coord. Chem. Rev.* **2003**, *245*, 167–175 and references cited therein.

[3] a) H. Petzold, S. Bräutigam, J. Windhager, W. Weigand, A. Majchrzak, G. Mloston, in *11th International Symposium on Inorganic Ring Systems* (Eds.: R. S. Laitinen, R. Oilunkaniemi), *Reports Series in Chemistry* **2006**, Oulu University Press, vol. 70, p. 62 (ISBN 9514281535); b) J. Windhager, M. Rudolph, S. Bräutigam, H. Görls, W. Weigand, *Eur. J. Inorg. Chem.* **2007**, 2748–2760; c) L. C. Song, Z. Y. Yang, Y. J. Hua, H. T. Wang, Y. Liu, Q.-M. Hu, *Organometallics* **2007**, *26*, 2106–2110; d) H. Alper, A. S. K. Chan, *Inorg. Chem.* **1974**, *13*, 232–263.

[4] a) A. Shaver, P. J. Fitzpatrick, K. Steliou, J. S. Butler, *J. Am. Chem. Soc.* **1979**, *101*, 1313–1315; b) C. Alvarez-Toledano, E. Delgardo, B. Donnadieu, E. Hernandez, G. Martin, F. Zamora, *Inorg. Chim. Acta* **2003**, *351*, 119–122.

[5] R. Seidel, B. Schautz, G. Henkel, *Angew. Chem. Int. Ed. Engl.* **1996**, *35*, 1710–1714.

[6] a) Y. Nicolet, A. L. de Lacey, X. Vernède, V. M. Fernandez, E. C. Hatchikian, J. C. Fontecilla-Camps, *J. Am. Chem. Soc.* **2001**, *123*, 1596–1601; b) Y. Nicolet, B. J. Lemon, J. C. Fontecilla-Camps, J. W. Peters, *Trends Biochem. Sci.* **2000**, *25*, 138–143; c) Y. Nicolet, C. Piras, P. Legrand, C. E. Hatchikian, J. C. Fontecilla-Camps, *Structure* **1999**, *7*, 13–23.

[7] a) X. Zhao, I. P. Georgakaki, M. L. Miller, J. C. Yarbrough, M. Y. Darensbourg, *J. Am. Chem. Soc.* **2001**, *123*, 9710–9711; b) F. Gloaguen, J. D. Lawrence, M. Schmidt, S. R. Wilson, T. B. Rauchfuss, *J. Am. Chem. Soc.* **2001**, *123*, 12518–12527; c) E. J. Lyon, I. P. Georgakaki, J. H. Reibenspies, M. Y. Darensbourg, *J. Am. Chem. Soc.* **2001**, *123*, 3268 –3278; d) M. Razavet, S. C. Davies, D. L. Hughes, J. E. Barclay, D. J. Evans, S. A. Fairhurst, X. Liu, C. J. Pickett, *Dalton Trans.* **2003**, 586 –595; e) J. D. Lawrence, H. Li, T. B. Rauchfuss, M. Benard, M.-M. Rohmer, *Angew. Chem. Int. Ed.* **2001**, *40*, 1768–1771; f) H. Li, T. B. Rauchfuss, *J. Am. Chem. Soc.* **2002**, *124*, 726–727; g) S. Ott, M. Kritikos, B. Åkermark, L. Sun, *Angew. Chem. Int. Ed.* **2003**, *42*, 3285–3288; h) C. Tard, X. Liu, S. K. Ibrahim, M. Bruschi, L. De Gioia, S. C. Davies, X. Yang, L.-S. Wang, G. Sawers, C. J. Pickett, *Nature* **2005**, *433*, 610–613; i) L.-C. Song, Z.-Y. Yang, H.-Z. Bian, Q.-M. Hu, *Organometallics* **2004**, *23*, 3082–3084; j) D. Seyferth, R. S. Henderson, L.-C. Song, *Organometallics* **1982**, *1*, 125–133; k) D. Seyferth, R. S. Henderson, L.-C. Song, *J. Organomet. Chem.* **1980**, *192*, C1; l) L.-C. Song, Z.-Y. Yang, H.-Z. Bian, Y. Liu, H.-T. Wang, X.-F. Liu, Q.-M. Hu, *Organometallics* **2005**, *24*, 6126–6135; m) M. Y. Darensbourg, E. J. Lyon, J. J. Smee, *Coord. Chem. Rev.* **2000**, *206–207*, 533–561; n) R. C. Linck, T. B. Rauchfuss, in *Bioorganometallics* (Ed.: D. Jaouen), Wiley-VCH, **2006**, 403–435; o) X. Zhang, C. Y. Chiang, M. L. Miller, M. V. Rampersad, M. Y. Darensbourg, *J. Am. Chem. Soc.* **2003**, *125*, 518–524; p) J. D.

Lawrence, H. Li, T. B. Rauchfuss, *Chem. Commun.* **2001**, 1482–1483; q) L. C. Song, J. Gao, H. T. Wang, Y. J. Hua, H. T. Fan, X. G. Zhang, Q. M. Hu, *Organometallics* **2006**, *25*, 5724–5729.
[8] a) , B. I. Kolobkov, A. I. Nekhaev, G. G. Aleksandrov, M. T. Tashev, Kh. B. Dustov, N. A. Parpiev, *Koord. Khim. Koord. Khim.* **1988**, *14*, 558–562; b) B. I. Kolobkov, A. I. Nekhaev, G. G. Aleksandrov, M. T. Tashev, Kh. B. Dustov, A. Ya. Sideridu, A. Ya. Seriya, *Khimicheskaya* **1987**, *4*, 953–954; c) A. Winter, L. Zsolnai, G. Huttner, *Z. Naturforsch., Teil B* **1982**, *37*, 1430–1436.
[9] H. Heimgartner, G. Mloston, J. Romanski, *Adamantanethione. Electronic Encyclopedia of Reagents for Organic Synthesis* (Ed.: L. A. Paquette), Article – RN 00504, John Wiley & Sons, New York, **2005**.
[10] G. Rindorf, L. Carlsen, *Acta Crystallogr., Sect. B* **1979**, *35*, 1179–1182.
[11] K. Eichkorn, O. Treutler, H. Oehm, M. Haeser, R. Ahlrichs, *Chem. Phys. Lett.* **1995**, *242*, 652–660.
[12] O. Treutler, R. Ahlrichs, *J. Chem. Phys.* **1995**, *102*, 346–354.
[13] K. Eichkorn, F. Weigend, O. Treutler, R. Ahlrichs, *Theor. Chem. Acc.* **1997**, *97*, 119–124.
[14] M. J. Frisch, G. W. Trucks, H. B. Schlegel, G. E. Scuseria, M. A. Robb, J. R. Cheeseman, J. A. Montgomery Jr, T. Vreven, K. N. Kudin, J. C. Burant, J. M. Millam, S. S. Iyengar, J. Tomasi, V. Barone, B. Mennucci, M. Cossi, G. Scalmani, N. Rega, G. A. Petersson, H. Nakatsuji, M. Hada, M. Ehara, K. Toyota, R. Fukuda, J. Hasegawa, M. Ishida, T. Nakajima, Y. Honda, O. Kitao, H. Nakai, M. Klene, X. Li, J. E. Knox, H. P. Hratchian, J. B. Cross, C. Adamo, J. Jaramillo, R. Gomperts, R. E. Stratmann, O. Yazyev, A. J. Austin, R. Cammi, C. Pomelli, J. W. Ochterski, P. Y. Ayala, K. Morokuma, G. A. Voth, P. Salvador, J. J. Dannenberg, V. G. Zakrzewski, S. Dapprich, A. D. Daniels, M. C. Strain, O. Farkas, D. K. Malick, A. D. Rabuck, K. Raghavachari, J. B. Foresman, J. V. Ortiz, Q. Cui, A. G. Baboul, S. Clifford, J. Cioslowski, B. B. Stefanov, G. Liu, A. Liashenko, P. Piskorz, I. Komaromi, R. L. Martin, D. J. Fox, T. Keith, M. A. Al-Laham, C. Y. Peng, A. Nanayakkara, M. Challacombe, P. M. W. Gill, B. Johnson, W. Chen, M. W. Wong, C. Gonzalez, J. A. Pople, *Gaussian 03*, Gaussian, Inc., Pittsburgh PA, **2003**.
[15] R. Heinzmann, R. Ahlrichs, *Theor. Chim. Acta* **1976**, *42*, 33–45.
[16] R. W. Rudolph, *Acc. Chem. Res.* **1976**, *9*, 446.
[17] D. M. P. Mingos, *Acc. Chem. Res.* **1984**, *17*, 311.
[18] F. Asinger, M. Thiel, G. Lipfert, *Justus Liebigs Ann. Chem.* **1959**, *627*, 195–212.
[19] H. Petzold, Diplomarbeit, FSU Jena, **2003**.
[20] G. Mloston, J. Romanski, H. Heimgartner, *Pol. J. Chem.* **1996**, *70*, 437–445.
[21] CCDC-640951 (for **3b**), -640952 (for **3c**), -640953 (for **3d**), -640954 (for **3e**), -640955 (for **4b**), -640956 (for **4d**), -640957 (for **4e**), -640958 (for **6b**), -640959 (for **6c**), -640960 (for **6d**), -640961 (for **7**) and -640962 (for **8**) contain the supplementary crystallographic data excluding structure factors. These data can be obtained free of charge from The Cambridge Crystallographic Data Centre via www.ccdc.cam.ac.uk/data_request/cif.
[22] *COLLECT*, Data Collection Software, Nonius B. V., Netherlands, **1998**.
[23] Z. Otwinowski, W. Minor, *Processing of X-ray Diffraction Data Collected in Oscillation Mode*, in *Methods in Enzymology*, vol. 276, Macromolecular Crystallography, Part A (Eds.: C. W. Carter, R. M. Sweet), Academic Press, New York, **1997**, pp. 307–326.
[24] G. M. Sheldrick, *Acta Crystallogr., Sect. A* **1990**, *46*, 467–473.
[25] G. M. Sheldrick, *SHELXL-97 (Release 97–2)*, University of Göttingen, Germany, **1997**.

Received: April 27, 2007
Published Online: August 10, 2007

